JBMR

ORIGINAL ARTICLE

Circulating Osteocalcin-Positive Cells as a Novel Diagnostic Biomarker for Bone Metastasis in Breast Cancer Patients

Kyung-Hun Lee,[1,2†] Kyoung Jin Lee,[3†] Tae-Yong Kim,[1,2] Febby Hutomo,[4] Hyun Jin Sun,[1] Gi Jeong Cheon,[4] Serk In Park,[3,5] Sun Wook Cho,[1] and Seock-Ah Im[1,2,6]

[1]Department of Internal Medicine, Seoul National University Hospital, Seoul, South Korea
[2]Cancer Research Institute, Seoul National University, Seoul, South Korea
[3]Department of Biochemistry and Molecular Biology, Korea University College of Medicine, Seoul, South Korea
[4]Department of Nuclear Medicine, Seoul National University College of Medicine, Seoul, South Korea
[5]Department of Medicine, Vanderbilt University School of Medicine, Nashville, TN, USA
[6]Department of Internal Medicine, Seoul National University College of Medicine, Seoul, South Korea

ABSTRACT

Current diagnosis of bone metastasis (BM) in breast cancer relies on structural changes of bone that occur only in the advanced stage. A sensitive biomarker for detecting early progression of bone metastasis is urgently required. We performed clinical and preclinical studies to investigate diagnostic value of circulating osteocalcin-positive cells (cOC) in breast cancer bone metastasis. Metastatic breast cancer patients ($n = 92$) with or without bone metastasis (ie, BM$^+$ or BM$^-$) were enrolled, and cOC were measured at enrollment. Patients were followed up for bone metastasis progression for 18 months. BM$^+$ patients ($n = 59$) were divided into progressive (PD) or stable disease (SD) groups, based on imaging studies at the end of the 18-month study. The PD group had higher baseline cOC compared with the SD group. Furthermore, higher cOC resulted in reduced BM progression-free survival. Three patients in the BM$^-$ group ($n = 33$) developed new BM during the 18-month study, and these patients had a higher level of baseline cOC compared with the remaining BM$^-$ patients. In murine preclinical studies, cOC increased at early time points when micro-metastases were evident only by histology but undetectable by bioluminescence imaging. Also, cOC levels predicted the progression of BM and correlated significantly with BM tumor burden. cOC increased in the early phase of breast cancer BM and can predict BM progression, supporting cOC as a potential novel biomarker. © 2020 American Society for Bone and Mineral Research.

KEY WORDS: BIOMARKER; BONE METASTASIS; BREAST CANCER; OSTEOBLASTS; OSTEOCALCIN

Introduction

Bone is the most frequent site of breast cancer metastasis, and skeletal-related events (SRE) of bone metastasis (BM) including pathologic bone fracture, spinal cord compression, hypercalcemia, and bone pain significantly affect the morbidities and mortalities of advanced-stage breast cancer patients.[1] Because previous SRE is a major risk factor for subsequent SRE, both primary and secondary preventions of SRE are attempted by using bone-targeting agents such as bisphosphonates and denosumab alone or in combination with chemotherapy and/or radiation.[2–4] However, the therapeutic efficacy and survival benefits of bone-targeting agents are limited.[5–9]

Therefore, earlier detection and intervention will be more beneficial for improving outcomes of bone metastasis.

The current standard assessment of bone metastasis is medical imaging such as whole-body bone scintigraphy (WBBS) and magnetic resonance imaging (MRI). WBBS is the most frequently used modality because it detects both osteoblastic and osteolytic lesions with strong sensitivity.[10,11] However, detectability of radionuclide activity in the WBBS depends on gross structural bone changes resulting from considerable progression of macro-metastasis. Moreover, flare phenomenon, referring to increased uptake in WBBS despite positive responses to treatment, is frequent in breast cancer, leading to misdiagnosis and erroneous changes in the treatment regimen.[12] The whole-

body MRI is the most sensitive method to detect cellular changes in bone but is not suitable for screening or routine follow-up checks. Therefore, sensitive and feasible diagnostic tools to detect the indolent or incipient micro-metastatic bone lesions are essential to benefit the clinical management of metastatic breast cancer patients.

Bone metastasis is commonly accompanied by bone destruction caused by the interactions among metastatic cancer cells, osteoclasts, and osteoblasts.[13] Although osteoclasts of hematopoietic lineage have long been considered the major effector cells and subsequent therapeutic target of tumor-induced osteolysis, increasing evidence supports that osteoblasts of mesenchymal stem cell lineage play central roles in the metastatic bone microenvironment regulating metastatic seeding, dormancy and awakening, osteolysis, and evasion of anti-tumoral immunity.[14,15] In particular, disseminating tumor cells first adhere to an osteoblastic niche and are then able to form a micro-metastatic tumor colony adjacently to the endosteal surface as shown by multiple preclinical models and patient sample biopsies.[16,17] Subsequently, during the initial phase of metastatic tumor outgrowth in bone, osteoblasts first become activated, proliferate, and release cytokines and growth factors essential to osteoclastogenesis, osteolysis, tumor growth, and anti-tumoral immunity.[18–21] These data collectively support that expansion and activation of osteoblasts are potentially the critical step for initiation and early progression of bone metastasis.

Circulating osteocalcin-positive cells (cOC) are small monocytic cells expressing osteocalcin (a late osteoblast differentiation marker) found within human peripheral blood mononuclear cells (PBMC). Khosla and colleagues demonstrated that adolescents who are in the active bone growth period have a higher level of cOC compared with adults.[22] Moreover, cOC also positively correlate with pathologic changes of bone turnover in such conditions as fracture, hypoparathyroidism, and diabetes.[23–28] These clinical observations collectively support that circulating osteoprogenitor cells reflect changes of bone turnover in either physiologic or pathologic status. Given that bone metastases, even in the phase of micro-metastasis, are more detrimental changes than any other pathologic changes of bone (eg, metabolic bone diseases), we thus hypothesized that cOC increase in the early phase of bone micro-metastasis, reflecting microscopic changes in the metastatic tumor microenvironment. The aim of this study was to investigate the difference of cOC in metastatic breast cancer with or without bone metastasis and to validate the predictive value of cOC in monitoring initiation and/or progression of bone metastasis.

Materials and Methods

Subjects and clinical study design

Women with metastatic breast cancer who visited Seoul National University Hospital, Seoul, South Korea, from July to September 2017 were enrolled, and clinical data including disease status of bone metastasis were collected over the 18-month study period. At the time of enrollment, the sites of metastasis were evaluated based on imaging studies and patients were divided into two groups according to the presence or absence of bone metastasis, designated BM$^+$ and BM$^-$ groups, respectively. Baseline bone scan images were reviewed by two experienced nuclear medicine physicians, and metastatic bone lesions were classified into three groups: no metastasis, low-burden, or high-burden metastasis groups. Patients with a single metastatic lesion were classified as low-burden group and patients with multiple and/or disseminated metastases were classified as high-burden group. All patients underwent blood sampling to measure cOC and bone turnover markers at the time of enrollment (ie, baseline cOC or bone turnover maker levels).

During the 18-month study, follow-up diagnostic imaging including bone scan was performed at least once every 6 months to screen or evaluate bone metastasis. Metastatic bone lesions were reevaluated at the 18-month point and classified as stable or progressive diseases. Progressive disease (PD) was defined as aggravated bone lesions or newly developed osteolytic bone lesions based on imaging studies or new SREs incidence during the 18-month follow-ups. All others were defined as stable disease (SD).

The study was approved by an institutional review board of Seoul National University Hospital (no. 1706-069-859), and all patients signed a written informed consent before enrollment. The study was conducted in accordance with the International Conference on Harmonization Good Clinical Practice guidelines and the provisions of the Declaration of Helsinki. The study was registered in the clinicaltrials.gov database (NCT03814811).

Flow cytometric analysis of human cOC

PBMCs were isolated by Ficoll-Paque density-gradient centrifugation of the whole blood samples collected in heparin-coated tubes. Cells were washed and suspended in phosphate-buffered saline supplemented with 2% fetal bovine serum and 2 mM EDTA (2×10^6 cells/200 μL), followed by staining with fluorochrome-conjugated monoclonal antibodies including anti-CD15 (clone HI98, BD Biosciences, San Jose, CA, USA), anti-CD34 (clone 8G12, BD Biosciences), and anti-osteocalcin (clone G-5, Santa Cruz Biotechnology, Dallas, TX, USA). Multicolor flow cytometry was performed using a three-laser 10-color BD FACSCanto, and analyzed with a BD FACS DIVA software. For analyzing cOC, CD15-negative cells were initially gated and CD34-negative, osteocalcin-positive cells were selected and defined as cOC (Fig. 1A).

Immunofluorescence staining and cell size analysis of cOC

PBMC were stained with fluorochrome-conjugated anti-CD34 (clone 8G12, BD Biosciences) and anti-osteocalcin antibodies (clone G-5, Santa Cruz Biotechnology) at 4°C for 30 minutes. The stained cells were smeared on a slide using a micropipettor tip and air-dried. Mounting media containing 4′,6-diamidino-2-phenyllindole (DAPI) was used to stain the nuclei. Fluorescence microscopic images were captured using a Leica (Buffalo Grove, IL, USA) TCS SP8 confocal laser-scanning microscope.

To measure cOC size, live PBMC were stained with anti-osteocalcin antibody conjugated with Alexa 647 and smeared on a slide glass. The slides were excited at 640 nm using light-emitting diode equipped in Smart Biopsy Cell Image Analyzer, a proprietary system of Cytogen, Inc. (Seoul, South Korea). The emitted light was collected at wavelength over 690 nm with a CCD camera. Images of individual cells were processed with an automatic cell counting program, also a proprietary technology developed by Cytogen, Inc. Cells larger than 5 μm in diameter and of circularity within a range between 0.8 and 1.3 were counted as cOC.

Clinical analysis of serum bone turnover markers

All serum samples were stored at −80°C until analysis. The serum bone formation marker, bone-specific alkaline phosphatase (bone ALP), was measured by chemiluminescence immunoassay
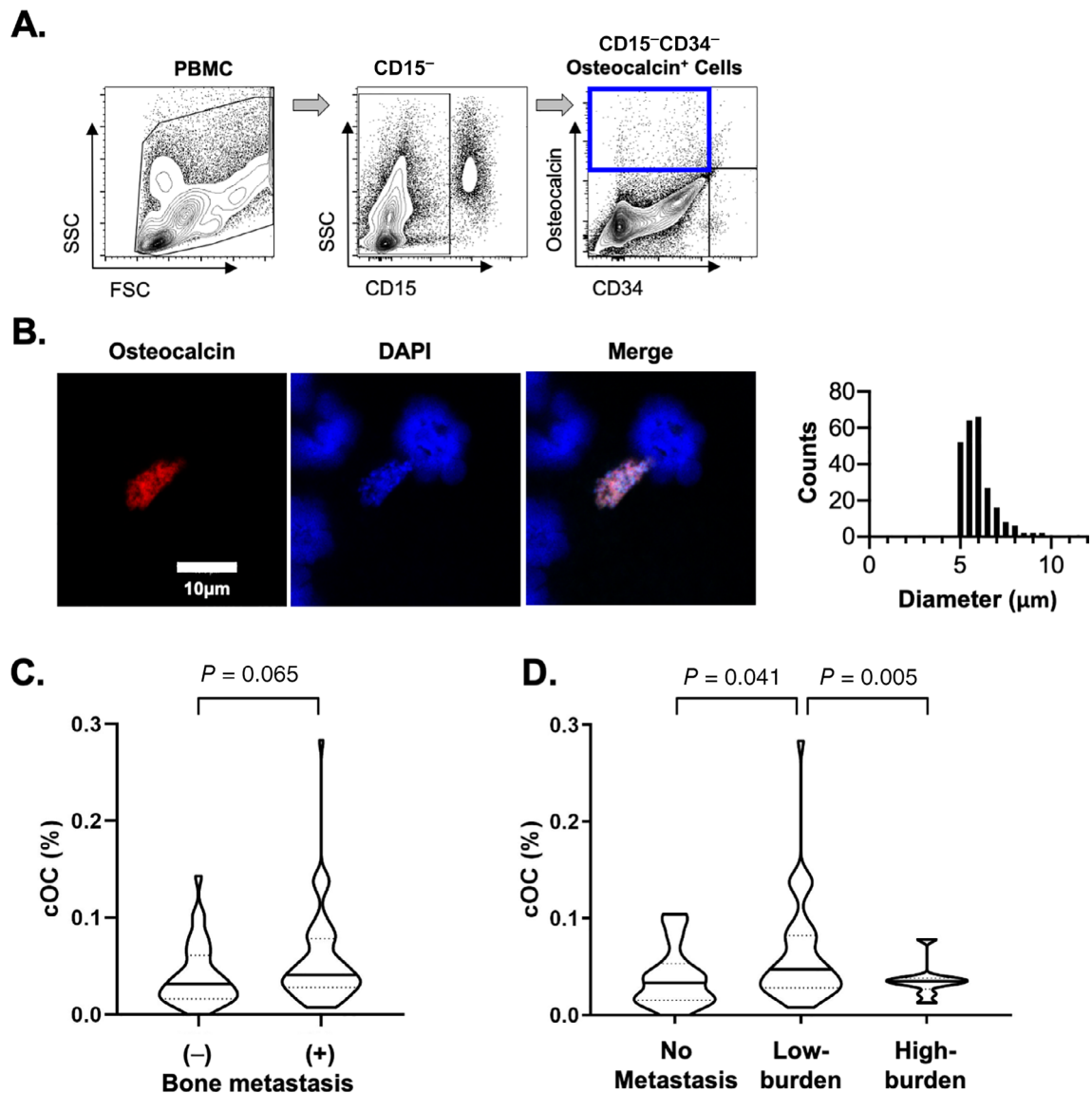
Fig. 1. cOC in the PBMC of metastatic breast cancer patients. (*A*) Representative contour plots of flow cytometric analyses showing gating strategy for cOC (CD15⁻CD34⁻Osteocalcin⁺ cells) in the PBMC. (*B*) Confocal microscopic images showing cOC stained with phycoerythrin-conjugated anti-osteocalcin antibody (red) and counterstained with DAPI (nucleus, blue) (×40 objective lens). A histogram of cOC cell size (diameter, μm) distribution. Approximately 120 cOC from two patient samples were analyzed by an automated single-cell image analysis system. (*C*) A violin plot comparing cOC % in metastatic breast cancer patient PBMC with (+) or without (−) bone metastasis. Horizontal lines represent median ± interquartile range. The *p* value was calculated by Mann–Whitney *U* test. (*D*) A violin plot comparing cOC % in metastatic breast cancer patient PMBC according to the metastatic activity in bone measured by whole-body bone scan. Patients were divided into three groups: no metastasis, low-burden, or high-burden metastasis. Horizontal lines represent median ± interquartile range. The *p* value was calculated by Mann–Whitney *U* test.

(Beckman Coulter, Brea, CA, USA) following manufacturer's instructions. A serum bone resorption marker, C-telopeptide of type I collagen, was measured by electrochemiluminescence immunoassay (Roche, Mannheim, Germany) following manufacturer's instructions.

Breast cancer cells

Luciferase-labeled human or murine breast cancer cells, MDA-MB-231-Luc or 4T1-Luc, respectively, were cultured in RPMI-1640 media containing 10% FBS and antibiotics in a 37°C 5% CO_2 incubator. A bone metastatic subclone of 4T1-Luc, termed 4T1-Bone, was established by repeating three rounds of in vivo intra-cardiac inoculation followed by harvesting bone metastatic cells in the hindlimb long bones after 7 to 21 days.[29,30] Increased bone metastatic potential was confirmed by in vivo bioluminescence quantitation of bone metastatic lesions in an intra-cardiac bone metastasis model (Supplemental Fig. S1). Cells were regularly confirmed free of mycoplasma by PCR and authenticated to match original or parental cell short tandem repeat (STR) profiles.

Bone metastasis in vivo models

Experimental bone metastasis mouse models were established by intra-tibial or intra-cardiac inoculation of breast cancer cells as described by Park and colleagues.[30] Briefly, breast cancer cells (1×10^5 MDA-MB-231-Luc or 1×10^4 4T1-Bone cells) were injected in the left heart ventricle (intra-cardiac injection) or in the proximal tibia (intra-tibial injection) of female athymic (for a human xenograft MDA-MB-231-Luc model) or Balb/c mice (for a murine syngeneic 4T1-Bone model) to model hematogenous metastasis or orthotopic bone tumor growth, respectively.[20,21] Subsequently, tumor growth was monitored by in vivo bioluminescence imaging as previously described.[20] All animal experiments were approved by the Institutional Animal Care and Use Committees of the Korea University College of Medicine (no. KOREA-2017-0114 and KOREA-2017-0160). All mice (Orient Bio, Seongnam, South Korea) were housed in a specific pathogen-free facility and fed a standard chow diet.

Flow cytometric analysis of murine cOC

Mice were anesthetized and blood was collected by cardiac puncture. Erythrocytes were lysed by ACK lysis buffer. Cells were washed and stained with fluorochrome-conjugated antibodies including anti-CD45 (clone 30-F11, BD Biosciences) and anti-osteocalcin (clone G-5, Santa Cruz Biotechnology), followed by flow cytometric analysis (BD FACSCanto II or Fortessa X-20). Gating strategy was described in Supplemental Fig. S2.

Histology

Decalcified, paraformaldehyde-fixed, and paraffin-embedded 4-μm thickness bone tissue sections were prepared for hematoxylin and eosin (H&E) staining and immunohistochemical analyses.[31] Briefly, antigen retrieval was performed by incubating in 0.1% Trypsin at 37°C for 30 minutes. Endogenous peroxidase activity was blocked by 3% H_2O_2 in PBS, and protein blocking was performed with 5% bovine serum albumin (BSA) in PBS. Rabbit anti-cytokeratin 8 primary monoclonal antibody (Clone EP1628Y, Abcam, Cambridge, UK; 1:500), biotinylated anti-rabbit secondary antibody (1:1000), HRP reagent, and 3,3′-diaminobenzidine were used to visualize the positively stained cytokeratin 8-positive tumor cells in bone. Representative histological images were captured using an EVOS FL Auto II cell imaging system. Tartrate-resistant acid phosphatase (TRAP) staining was performed as previously described.[32]

Statistical analysis

Clinical data are presented as mean $\pm$ SD or median [minimum-maximum]. Student's t test, one-way ANOVA, and chi-square test were used to compare groups. Statistical analysis was performed using IBM (Armonk, NY, USA) SPSS statistics software version 21.0. Progression-free survival (PFS) of bone metastasis was defined as the time from enrollment until the date of objective disease progression in bone or death from any cause in the absence of progression. Both PFS and overall survival (OS) were estimated in all enrolled patients by log-rank test using one-sided significance level of 0.01. For mouse preclinical data, statistical analysis was performed using GraphPad (La Jolla, CA, USA) Prism Version 8.0. Mann–Whitney U test was used to compare differences between two groups, and one-way ANOVA with Tukey post hoc multiple comparisons test was used to compare pairwise differences among multiple groups. Polynomial regression analysis was performed to determine quadratic trends between time (days) versus cOC (%) or bioluminescence activity. All statistical analyses for preclinical data were two-sided, and p values were rounded up to the third decimal.

Results

Baseline characteristics of patients with or without bone metastasis

A total of 92 females with metastatic breast cancer were enrolled. The mean ages (years) at diagnosis and at enrollment were 49.2 ± 9.0 and 55.0 ± 8.9, respectively. Fifty-nine (64%) patients had bone metastasis, including 13 (14%) patients with bone-only metastasis and 46 (50%) patients with metastasis at bone plus extraskeletal sites. Table 1 shows clinical characteristics of the patients according to the presence of bone metastasis. The bone-only metastasis group showed younger age at the time of breast cancer diagnosis and less frequent postmenopausal status than the bone plus extraskeletal sites group or the extraskeletal sites-only metastasis group. Distribution of subtypes of breast cancer was significantly different between the groups. Hormone receptor (HR)- and/or HER2-positive subtypes were 100% and 97% in bone-only and bone plus extraskeletal sites metastasis groups, respectively, whereas only 64% in the extraskeletal sites-only metastasis group were HR-positive. Among 26 patients who received zoledronate for bone metastasis, 13 patients received the drug within 2 years from the enrollment, and 3 of them received the drug immediately before enrollment. Eight patients had previously received radiation therapy for bone lesions at least 1 year before enrollment, but there was no patient who received radiation therapy within 1 year.

The percentage of cOC is higher in the patients with early bone metastasis

At the time of enrollment, the percentage of cOC in the CD15$^-$ PBMC was analyzed by flow cytometric analyses (Fig. 1A). Combinations of surface markers defining cOC are different among investigators (reviewed and summarized in Feehan and colleagues.[33] Because this is the first study of cOC in cancer patients, we utilized a more inclusive combination of markers and defined cOC as CD15$^-$CD34$^-$Osteocalcin$^+$ cells. The stained cells were visualized under a confocal scanning laser microscope, and the size of cOC was measured using an automated image analysis tool (Fig. 1B). The average size of cOC was 5.8 ± 1.0 μm (Fig. 1B). The median percentage of cOC in the PBMC was 0.03% (0.00–0.14%), and cOC was higher in patients with bone metastasis than those without bone metastasis with marginal significance (0.04% [0.01–0.28%] versus 0.03% [0.00–0.14%], $p = 0.065$; Fig. 1C). Serum bone turnover markers, including bone-specific ALP and C-telopeptide, showed no difference among the groups (Supplemental Table S1).

Because all enrolled patients were in various stages of bone metastasis, patients were further divided by baseline bone scan images and classified into three groups according to their metastatic activity in bone: no metastasis, low-, and high-burden metastasis, respectively. Interestingly, patients with low-burden metastasis showed higher cOC than those with no metastasis or high-burden metastasis (Fig. 1D). Next, the relationship between cOC and fracture in both BM$^-$ and BM$^+$ was analyzed, since fracture alters bone structures and potentially plays a role

Table 1. Baseline Characteristics According to the Presence of Bone Metastasis

| | Bone metastasis (+) | | Bone metastasis (−) | |
| | Bone-only | Bone plus extraskeletal sites | Extraskeletal sites only | |
	n = 13	n = 46	n = 33	p Value
Age (years) at enrollment	54.8 ± 7.6	54.1 ± 10.2	56.4 ± 6.8	0.509
At diagnosis				
Age (years)	44.0 ± 6.2	49.3 ± 10.3	51.2 ± 7.6	0.051
Postmenopausal, n (%)	4 (31)	24(52)	23 (70)	0.044
Molecular subtypes				0.001
ER/PR(+) HER2(+), n (%)	1 (8)	7 (15)	6 (18)	
ER/PR(+) HER2(−), n (%)	11 (84)	28 (61)	9 (27)	
ER/PR(−) HER2(+), n (%)	1 (8)	8 (17)	6 (18)	
ER/PR(−) HER2(−), n (%)	0	3 (7)	12 (36)	
Previous use of zoledronate, n (%)	6 (46)	20 (43)		1.000
Previous radiotherapy to bone, n (%)	2 (15)	6 (13)		1.000

ER/PR(+) = estrogen receptor (ER)-positive and/or progesterone receptor (PR)-positive; ER/PR(−) = ER-negative and PR-negative.

in mobilizing cOC. Among 59 BM$^+$ patients, 4 patients who had fracture at metastatic bone showed higher cOC than those who did not experience fracture, but statistical significance was not observed (0.09% [0.03–0.28%] versus 0.04% [0.01–0.14%], p = 0.176; Supplemental Fig. S3). In contrast, 4 patients among 33 BM$^−$ patients had benign-looking fracture on bone scintigraphy, and their cOC level was similar to that of BM$^−$ patients without fractures (Supplemental Fig. S3). Taken together, cOC was significantly increased in the early phase of bone metastasis, and benign-looking fracture did not affect metastasis-related increase of cOC.

The percentage of cOC predict progression of bone metastasis

Subsequently, we aimed to examine whether cOC measured at enrollment were able to predict disease progression of bone metastasis. At the end of our 18-month study, disease status of metastatic bone lesions was reevaluated and classified as stable disease (SD) or progressive disease (PD) groups. Twenty-two (37%) patients showed PD and 37 (63%) patients showed SD. Interestingly, cOC, measured at baseline, were significantly higher in the PD than the SD group (0.08 ± 0.03% versus 0.04 ± 0.04%, p < 0.001; Fig. 2A), whereas serum bone turnover markers such as C-telopeptide and bone-specific ALP (also measured at baseline) showed no difference (Table 2). Other clinical characteristics such as initial stage of disease or hormone receptor status showed no differences between groups (Table 2). Based on ROC analysis, area under ROC curves was 0.907 (p < 0.001), and the optimal cut-off value was established at 0.045% with the highest positive predictive value, 100% (Fig. 2B). Furthermore, 59 BM$^+$ patients were divided into two groups by cOC = 0.045% and bone metastasis PFS were analyzed. The patients with cOC ≥0.045% showed significantly shorter bone metastasis PFS than those with cOC <0.045% (hazard ratio [HR] = 4.79, p < 0.001, log-rank test; Fig. 2C).

Higher cOC predict de novo bone metastasis in the patients without bone metastasis at baseline

Among 33 patients of extraskeletal site-only metastasis, 3 patients developed de novo bone metastasis (designated incipient BM$^+$) during the 18-month follow-up. The median time

from enrollment to the diagnosis of de novo bone metastasis was 9 (9–15) months. The age at diagnosis was significantly higher in the incipient BM$^+$ group than the BM$^−$ group (57.7 years ± 3.5 versus 50.6 years ± 7.6, p = 0.041), whereas other clinical characteristics such as initial stage of disease or hormone receptor status showed no difference (Table 3). Two patients had metastases in the axial skeleton, and 1 patient had a single bone metastasis in the femur. Remarkably, baseline cOC was significantly higher in the incipient BM$^+$ group than the BM$^−$ group (0.08 ± 0.04% versus 0.03 ± 0.02%, p < 0.001; Table 3 and Fig. 3A), whereas serum bone turnover markers showed no significant difference between groups (Table 3). Logistic regression analysis was performed with related variables, including age at diagnosis, cOC, bone-specific ALP, and C-telopeptide, and identified cOC as an independent risk factor for incipient bone metastasis (Supplemental Table S2).

To further evaluate predictive value of cOC for the progression of bone metastasis, a ROC curve analysis was performed. Area under ROC curves was 0.956 (p = 0.01), and the optimal cut-off value was established at 0.069% with the highest positive predictive value, 100% (Fig. 3B). Patients with cOC ≥0.069% showed significantly shorter bone metastasis-free survival than those with cOC <0.069% (HR = 462.5, p < 0.001; Fig. 3C). Collectively, higher baseline cOC predict the development of new bone metastasis in the patients without overt clinical bone metastasis at enrollment.

Increase of cOC precedes the outgrowth of bone micro-metastasis and tumor-induced osteolysis in mouse bone metastasis models

To further explore the kinetics of cOC changes during the progression of bone metastasis from micro-metastasis to massive osteolysis, mouse models of bone metastasis were established, and cOC were measured at multiple time points. First, MDA-MB-231-Luc human breast cancer cells were xenografted in the proximal tibias of female athymic mice, and tumor cell colonization and growth were examined by bioluminescence imaging and histologic analyses at days 3, 5, 11, and 14 (Fig. 4A). Tumors became detectable by bioluminescence imaging only at day 14, but histological examination confirmed the existence of tumors at earlier time points (ie, days 3, 5, and 11) (Fig. 4C, D). Tumor cells formed micro-metastatic colonies adjacently to the
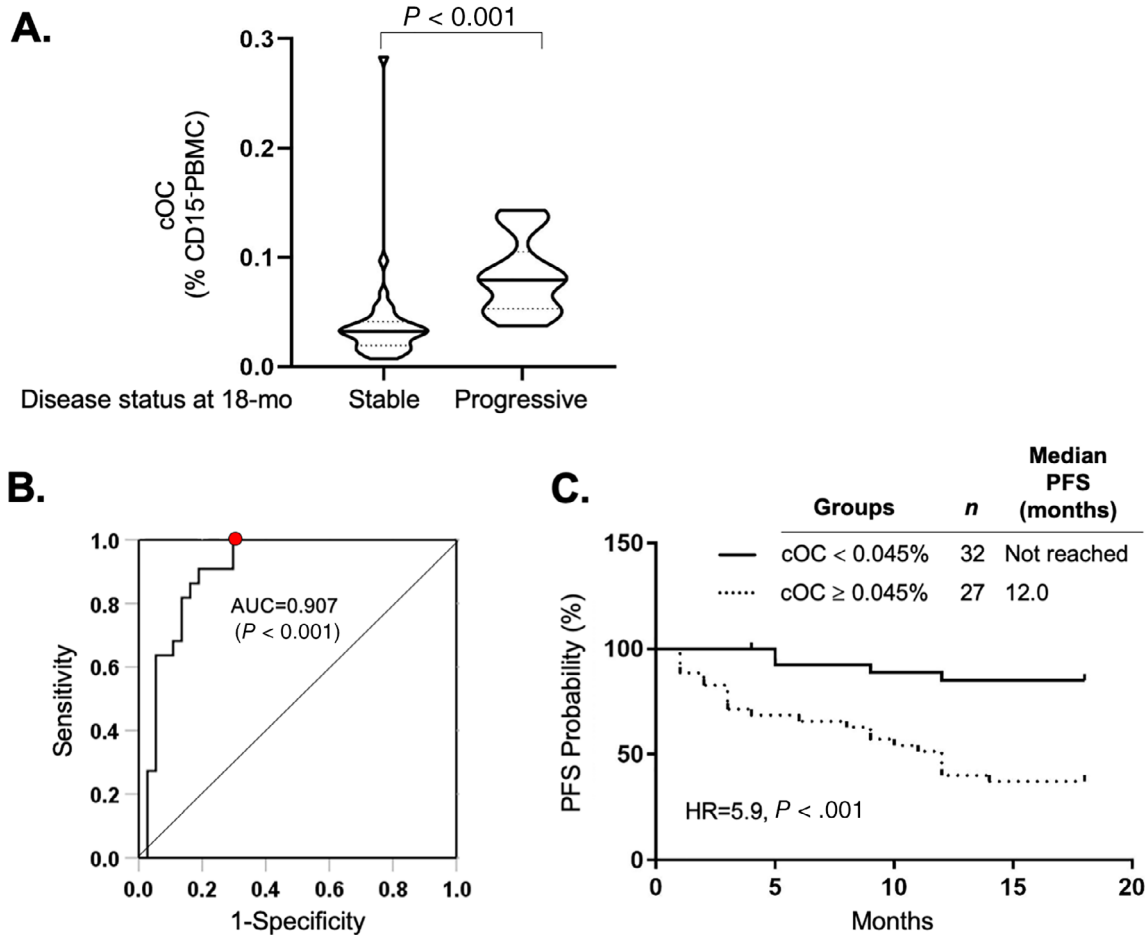
Fig. 2. cOC predicts the progression of established bone metastasis. Sixty-three patients with bone metastasis were sampled for cOC analysis at baseline and reevaluated for disease progression after 18 months by diagnostic imaging study. The patients were divided into two groups, ie, stable ($n = 37$) and progressive ($n = 22$) based on diagnostic images. (A) A violin plot showing cOC % measured at baseline between stable and progressive disease groups. (B) A ROC curve for the evaluation cOC cut-off value for the progression of established bone metastasis. (C) Kaplan–Meier survival analysis for bone metastasis-free survival between two groups dichotomized by cOC percentage (cut-off = 0.045%). Survival analysis was performed by log-rank test.

Table 2. Clinical Characteristics of Patients With Bone Metastasis (BM⁺) According to the Disease Status of Bone Metastasis at the End of 18-Month Study

Disease status of bone metastasis	Stable disease	Progressive disease	p Value
No. of patients	37	22	
Age (years) at enrollment	53.5 ± 10.5	55.6 ± 8.1	0.417
At diagnosis			
Age (years)	47.4 ± 10.6	49.4 ± 8.0	0.447
Postmenopausal, n (%)	19 (51)	9 (41)	0.436
Molecular Subtypes			0.361
ER/PR(+) HER2(+), n (%)	7 (19)	1 (4)	
ER/PR(+) HER2(−), n (%)	22 (60)	17 (77)	
ER/PR(−) HER2(+), n (%)	6 (16)	3 (14)	
ER/PR(−) HER2(−), n (%)	2 (5)	1 (5)	
Previous use of zoledronate, n (%)	13 (35)	13 (59)	0.073
Previous radiotherapy to bone, n (%)	4 (11)	4 (18)	0.430
C-telopeptide (ng/mL)	0.33 ± 0.26	0.35 ± 0.19	0.721
Bone ALP (μg/L)	18.1 ± 15.6	15.8 ± 7.5	0.554

ER/PR(+) = estrogen receptor (ER)-positive and/or progesterone receptor (PR)-positive; ER/PR(−) = ER-negative and PR-negative; Bone ALP = bone-specific alkaline phosphatase.

Table 3. Clinical Characteristics of Patients Without Bone Metastasis (BM⁻) According to the Presence of Incipient (De Novo) Bone Metastasis at the End of 18-Month Study

Presence of incipient bone metastasis at 18 months	BM⁻	Incipient BM⁺	p Value
No. of patients	30	3	
Age (years) at enrollment	56.0 ± 6.9	60.7 ± 4.0	0.168
At diagnosis			
Age (years)	50.6 ± 7.6	57.7 ± 3.5	0.041
Postmenopausal, n (%)	20 (67)	3 (100)	0.130
Molecular subtypes			0.274
ER/PR(+) HER2(+), n (%)	5 (17)	1 (33)	
ER/PR(+) HER2(−), n (%)	9 (30)	0 (0)	
ER/PR(−) HER2(+), n (%)	6 (20)	0 (0)	
ER/PR(−) HER2(−), n (%)	10 (33)	2 (67)	
C-telopeptide (ng/mL)	0.38 ± 0.23	0.58 ± 0.59	0.619
Bone ALP (µg/L)	20.6 ± 22.1	11.7 ± 2.6	0.052

ER/PR(+) = estrogen receptor (ER)-positive and/or progesterone receptor (PR)-positive; ER/PR(−) = ER-negative and PR-negative; Bone ALP = bone-specific alkaline phosphatase.

endosteal surface in the bone marrow as early as days 3 and 5 (Fig. 4D). At day 11, expansion of tumor growth was prominent, and woven bone formation (indicating increased osteoblastic activity) mixed with tumor cells was observed (Fig. 4D). On day 14, tumor cells had nearly completely replaced the bone marrows, and lytic bone lesions were observed. Interestingly, cOC significantly increased at days 5 and 11 compared with non-tumor-bearing control mice (Fig. 4B), suggesting that increase of cOC precedes the outgrowth of bone micro-metastasis and the increase is indicative of the existence or development of bone metastasis. Moreover, polynomial regression analyses revealed that tumor growth was exponential (blue dotted line, Fig. 4C), whereas cOC levels increased in early bone metastasis (ie, day 5) and subsequently taper off (blue dotted quadratic trend line, Fig. 4B) in the massive osteolysis phase, supporting the value of cOC as an early bone metastasis biomarker.

Increase of cOC in the early phase of bone metastasis progression even when the metastatic lesions are not detectable by bioluminescence

To further investigate cOC kinetics in a more clinically relevant hematogenous bone metastasis model, an intra-cardiac injection bone metastasis model was used. MDA-MB-231-Luc cells were injected in the systemic circulation via the left heart ventricle of female athymic nude mice and the development of bone metastasis was monitored by bioluminescence imaging every 3 to 4 days (Fig. 5A). Increase of cOC was observed as early as day 7 (Fig. 5B), whereas bioluminescence imaging could not detect bone metastasis until day 22 (Fig. 5C). In addition, similar to the intra-tibial model (Fig. 4B), cOC levels showed a significant quadratic trend (Fig. 5B).

Furthermore, we employed an additional mouse model to validate our data. Briefly, intra-cardiac injection of 4T1-Bone, a bone metastatic subclone of 4T1 murine breast cancer cells, commonly results in 70% to 80% success in forming bone metastasis in hindlimb long bones (Supplemental Fig. S1), and we took advantage of this heterogeneity. Among 15 mice injected with 4T1-Bone cells, 11 mice developed overt bone metastasis (73%) but 4 mice did not form bioluminescence-detectable bone metastasis (27%) by day 9 (Fig. 6A). In contrast, cOC levels distinguished BM⁺ and BM⁻ groups as early as day 6 when bioluminescence imaging failed to distinguish the two groups (Fig. 6B).

Furthermore, cOC positively correlated with the intensity of bioluminescence on day 9 ($\gamma^2 = 0.425$, $p < 0.01$) (Fig. 6C). Taken together and consistent with our human data, the current mouse study confirmed that cOC changes in the early phase of bone metastasis of breast cancer and also that cOC are a predictive biomarker for bone metastasis progression.

Discussion

One of the urgent unmet clinical needs for bone metastasis is an early diagnosis before the initiation of the destructive cascades of bone tissue. The present study developed a blood test to predict and monitor the progression of bone metastasis. We demonstrated that level of cOC to predict the de novo development of bone metastasis in metastatic breast cancer patients, earlier than the current image-based diagnosis. The optimal cut-off value for cOC predicting de novo development of bone metastasis was 0.069% by flow cytometric analysis of PBMC. Furthermore, higher cOC also predict disease progression in already established bone metastasis. Patients with cOC higher than a 0.045% cut-off showed significantly shorter bone metastasis progression-free survival. In contrast, serum bone turnover markers, including bone-specific ALP and C-telopeptide, did not show significant difference during the progression of bone metastasis, indicating limitations of serum bone turnover markers as effective diagnostics for early lesions of bone metastasis. Taken together, the present study for the first time to our knowledge demonstrates that cOC are a potentially sensitive novel biomarker for early diagnosis of bone metastasis in breast cancer patients.

For the purpose of early diagnosis of de novo bone micrometastasis or reactivation of subsistent bone metastasis in optimizing the starting point of interventions, previous studies have been focused on developing novel biomarkers using bone turnover-related markers or various cancer-related factors.[34] First, bone turnover-related markers such as bone-specific ALP, P1NP, C-telopeptide, or N-telopeptide have been intensively investigated for diagnostic and prognostic tools;[35] however, most of the investigations were retrospective, and the predictive values were suboptimal. In general, measuring bone turnover-related markers has several limitations. The serum levels easily change depending on the circadian and seasonal variations,
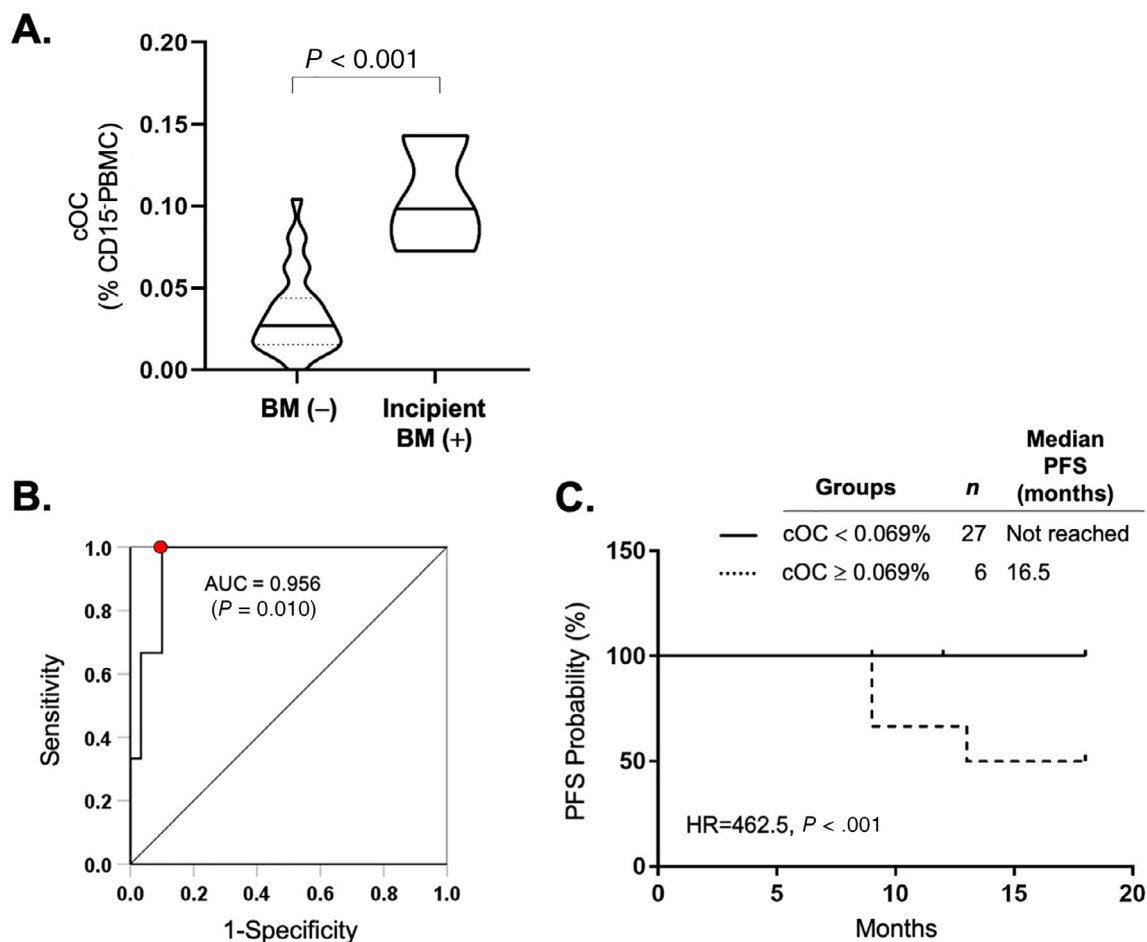
Fig. 3. Higher cOC predict de novo bone metastasis in the patients without bone metastasis at baseline. Thirty-three patients without bone metastasis were sampled for cOC analysis at baseline and reevaluated for disease progression after 18 months by diagnostic imaging study. The patients were divided into two groups according to the presence of bone metastasis at 18 months, ie, no bone metastasis (BM⁻, $n = 30$) and incipient bone metastasis (BM⁺, $n = 3$). (*A*) A violin plot showing cOC % measured at baseline between BM⁻ and incipient BM⁺ patient PBMC. (*B*) A ROC curve for the evaluation cOC cut-off values for incipient bone metastasis. (*C*) Kaplan–Meier survival analysis for bone metastasis-free survival between two groups dichotomized by cOC percentage (cut-off = 0.069%). Survival analysis was performed by log-rank test.

fasting status, and liver and kidney functions.[36] In particular, anti-cancer therapies including hormone therapies to breast or prostate cancers affect circulating levels of bone turnover-related markers. To overcome these shortcomings, studies proceeded to investigate cancer-related proteins, such as IL-1β, growth/differentiation factor (GDF)-15, CXCR-4, osteopontin or parathyroid hormone (PTH)-related peptide (PTHrP), or several miRNAs were suggested as biomarkers for bone metastasis.[37–40] However, these also presented several limitations. First, the above-listed candidate markers were investigated using metastatic tissue samples with retrospective review of clinical data, undermining clinical usefulness as non-invasive diagnostic tools. Second, most of the markers were not specific to bone metastasis and could have been affected by extraskeletal metastatic lesions or systemic inflammation. Thus, previous efforts highlight the need to identify novel predictive biomarkers.

In the current study, a cross-sectional comparison of cOC at enrollment between the patients with and without bone metastasis

showed minimal differences despite statistical significance. One of the possible explanations is that the recruited patients with bone metastasis (BM⁺) were in various stages of bone metastasis, and 25% and 13% of them had already received bone-targeting treatments such as intravenous zoledronic acid or radiation therapy to bone. Indeed, bone scan analysis showed that the levels of cOC were significantly higher in the low-burden group (which can now be interpreted as early bone metastasis) compared with the high-burden group, who had disseminated bone metastasis (ie, advanced bone metastasis). Interestingly, cOC in the high-burden group was similar to that in the no-metastasis group. Concurringly, our animal experiment using the intra-tibial injection model showed that levels of cOC increased at the early micro-metastasis stage when micro-metastatic bone lesions are involved with osteoblastic proliferation and mobilization but reduced in the subsequent phase of massive osteolysis and expansive tumor growth (Figs. 4 and 5). Collectively, presence of cOC predicted early incidence of micro-metastasis in bone more accurately than the changes of bone turnover markers, whereas cOC decreased correlatively in the later

stage of advanced-stage (osteolytic) bone metastasis. This study led us to deduce that measurement of cOC, in addition to imaging diagnostics, can first be applied as a sensitive novel diagnostic for early detection of initiation or reactivation of bone metastasis. For example, the patients with higher cOC but no clear evidence of bone metastasis on imaging diagnostics can be recommended for short-interval follow-up or considered for further preventive therapy using high-dose antiresorptives. Further prospective studies are needed to validate the predictive values of cOC in stages II and III patients with clinically high risk for bone metastasis and the value of cOC as companion diagnostics with bone-targeting therapeutics such as zoledronate or denosumab.
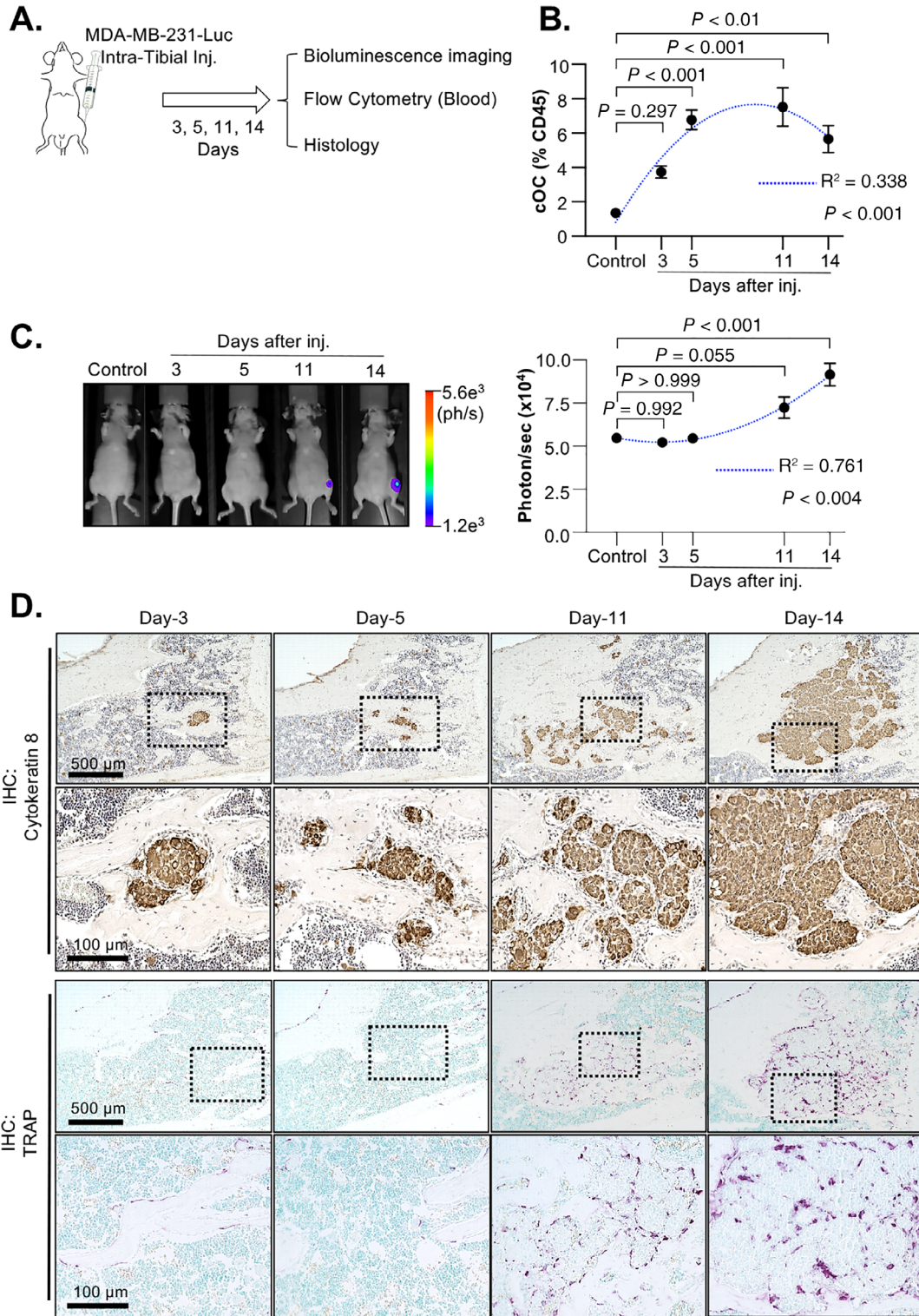

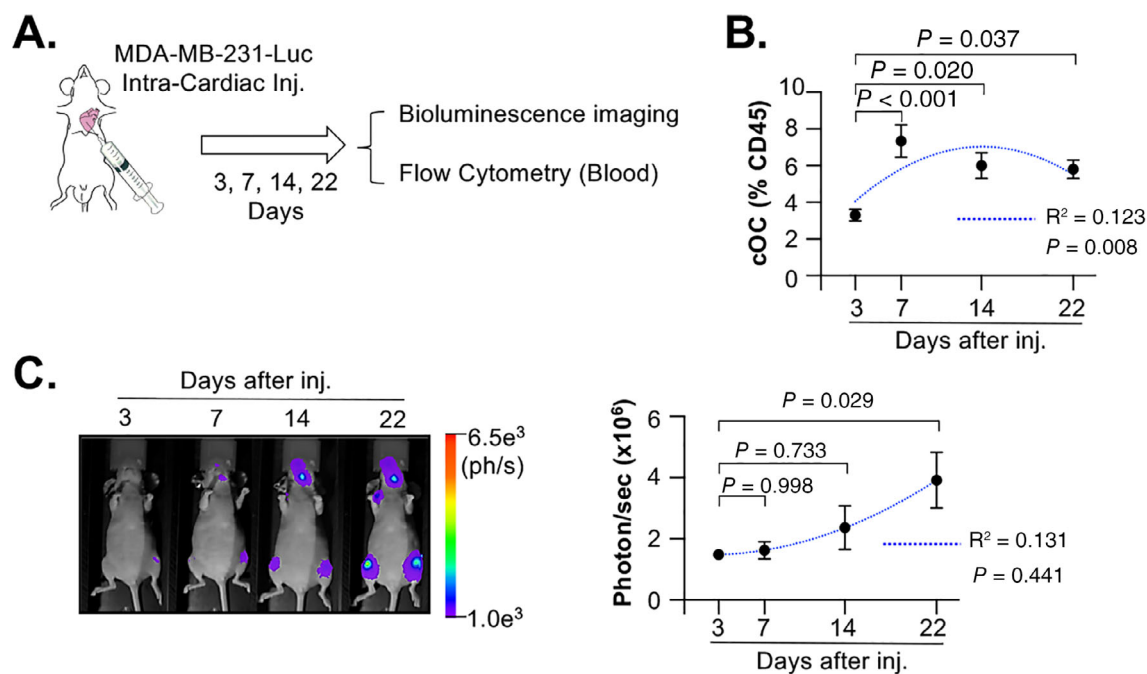**Fig. 4.** Legend on next page.

Fig. 5. cOC increase in the early phase of bone metastasis progression even when the metastatic lesions are not detectable by bioluminescence imaging. (*A*) Schematic representation of the experiment. To model hematogenous metastasis to bone, MDA-MB-231-Luc human breast cancer cells were injected into the systemic circulation via left ventricular (ie, intra-cardiac) injection. At days 3, 7, 14, and 21 after tumor inoculation, bone metastasis was evaluated by bioluminescence imaging, and subsequently mice were euthanized for histological analysis and blood sampling for flow cytometry. $n = 18$ per each time point group. (*B*) cOC (% of total CD45 cells) were quantified by FACS from whole blood and plotted. Data are mean $\pm$ SEM. The *p* values are from Tukey post hoc multiple comparisons analysis. The *p* values comparing each point with day 3 group are indicated, and not-shown *p* values are: day 7 versus day 14 $p = 0.463$; day 7 versus day 22 $p = 0.335$; day 14 versus day 22 $p = 0.996$. Polynomial regression analysis (blue dotted line) revealed a significant quadratic trend between time (day) versus cOC (%) ($R^2 = 0.123$, β2 coefficient $p = 0.008$). (*C*) Representative pictures of bioluminescence imaging at each time point and a graph showing quantification of bone metastasis lesion size. Data are mean $\pm$ SEM. The *p* values are from Tukey post hoc multiple comparisons analysis. The *p* values comparing each point with day 3 group are indicated, and not-shown *p* values are: day 7 versus day 14 $p = 0.823$; day 7 versus day 22 $p = 0.044$; day 14 versus day 22 $p = 0.271$. Polynomial regression analysis (blue dotted line) did not show quadratic trend between time (day) versus bioluminescence activity ($R^2 = 0.131$, β2 coefficient $p = 0.441$).

Fracture is one of the confounding factors during the diagnosis of bone metastasis, since metastatic breast cancer patients, especially those who underwent aromatase inhibitor therapy, have high risk for benign osteoporotic fracture.[41] Once patients have a fracture, it is difficult to distinguish between benign osteoporotic fractures versus metastasis-related fractures. Moreover, fractures cause significant changes in bone structure; hence it is reasonable to deduce that cOC might be increased with fracture independently of bone metastasis. The present study showed that cOC were not significantly different according to the presence of the fracture.

FIGURE 4 Increase of cOC precedes the outgrowth of bone micro-metastasis and the tumor-induced osteolysis in vivo. (*A*) Schematic representation of the experimental design. MDA-MB-231-Luc human breast cancer cells were implanted in the proximal tibia of female athymic mice. At days 3, 5, 11, and 14 after tumor inoculation, bone metastasis was evaluated by bioluminescence imaging, and subsequently mice were euthanized for histology and blood sampling for flow cytometry. Non-tumor mice were used as controls. (*B*) cOC (% of total CD45 cells) were measured by flow cytometric analysis of PBMC. Data are mean $\pm$ SEM. The *p* values are from Tukey post hoc multiple comparisons analysis. The *p* values comparing each point with control group (ie, non-tumor group) are indicated, and not-shown *p* values are: day 3 versus day 5 $p = 0.031$; day 3 versus day 11 $p = 0.004$; day 3 versus day 14 $p = 0.347$; day 5 versus day 11 $p = 0.945$; day 5 versus day 14 $p = 0.818$; day 11 versus day 14 $p = 0.379$. $n = 8$ (control group), 15 (days 3, 5, 11 groups), and 14 (day 14 group). Polynomial regression analysis (blue dotted line) revealed a significant quadratic trend between time (day) versus cOC (%) ($R^2 = 0.338$, β2 coefficient $p < 0.001$). (*C*) Representative pictures of bioluminescence imaging and a graph showing quantification of bone metastasis lesion size. Data are mean $\pm$ SEM. The *p* values are from Tukey post hoc multiple comparisons analysis. The *p* values comparing each point with control group (ie, non-tumor group) are indicated, and not-shown *p* values are: day 3 versus day 5 $p = 0.995$; day 3 versus day 11 $p = 0.022$; day 3 versus day 14 $p < 0.001$; day 5 versus day 11 $p = 0.049$, day 5 versus day 14 $p < 0.001$; day 11 versus day 14 $p = 0.033$. $n = 5$ each group. Polynomial regression analysis (blue dotted line) revealed a significant positive quadratic trend between time (day) versus bioluminescence activity ($R^2 = 0.761$, β2 coefficient $p = 0.004$). (*D*) Representative pictures from histological examination of the tumor-bearing bones. Bone metastatic tumors were detected by anti-human cytokeratin 8 immunohistochemistry, and tumor-induced osteoclastogenesis was visualized by TRAP staining. Upper row = lower magnification; lower row = higher magnification of the insets (dotted boxes).
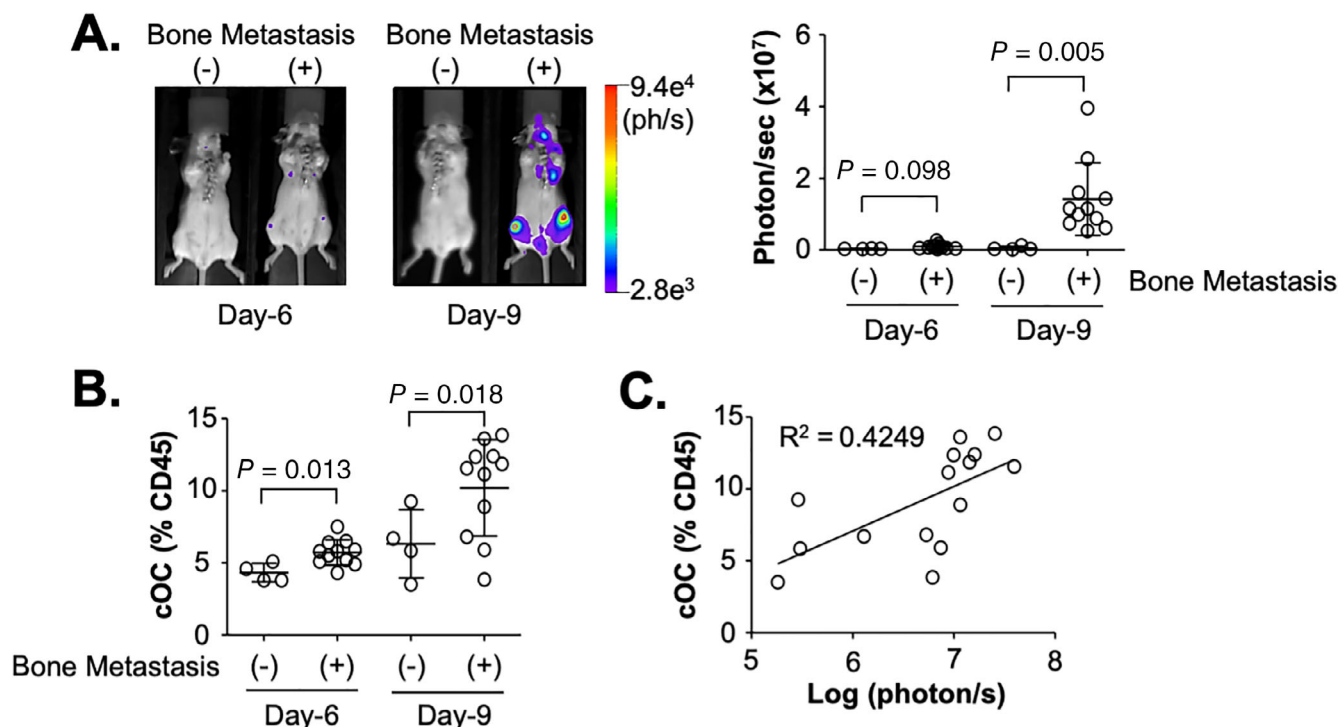
Fig. 6. cOC levels predict the development of bone metastasis in vivo. A murine syngeneic bone metastasis model was established by injecting the bone metastatic subclone of 4T1 breast cancer cells (ie, 4T1-Luc-Bone) in the systemic circulation of female Balb/c mice ($n = 15$). (*A*) Eleven mice developed bone metastasis within 9 days as determined by bioluminescence imaging (ie, bone metastasis[+] group), whereas the other 4 mice did not (ie, bone metastasis[−] group). The incidence of bone metastasis development in this model was within the normal range based on previous experiments in our laboratory. Representative bioluminescence images were chosen from each group. Quantification of bioluminescence signals confirmed the development of bone metastasis. Dots represent individual mice, and whiskers represent median ± interquartile range. The *p* values are from Mann–Whitney *U* test. (*B*) cOC (% of total CD45 cells) were significantly increased in the bone metastasis group at day 6 when bioluminescence activity between the two groups were not significant. Dots represent individual mouse, and whiskers represent median ± interquartile range. The *p* values are from Mann–Whitney *U* test. (*C*) Linear regression analysis between cOC and bone metastasis tumor size measured by bioluminescence activity on day 9.

Particularly, cOC in the BM[−] group showed no difference between groups whether they had fracture or not, suggesting that benign fractures do not affect cOC levels. Meanwhile, BM[+] patients with metastatic site fracture showed higher cOC than patients without fracture in the BM[+] group, although it was not statistically significant because of the small sample size. Indeed, the impact of fractures on cOC levels needs further investigation to increase sample size and also consider the effects of onset time of fractures.

Although the current study focused only on breast cancer bone metastasis, we anticipate that cOC can be applicable to bone metastasis from other organs such as prostate, lung, etc. Prostate cancer also frequently metastasizes to bone but predominantly forms osteoblastic lesions, contrary to osteolytic lesions formed by breast cancer cells. Importantly, many clinical features such as hormone levels, hormone receptors, postmenopausal osteoporosis, and osteoblastic activities must be taken into account when conducting future clinical trials using cOC in prostate and lung cancer bone metastases.

In conclusion, higher levels of cOC in PBMC can predict incipient progressions of bone metastasis in breast cancer earlier than imaging modalities. Measurement of cOC may serve as a sensitive novel biomarker for early diagnosis and progression of bone metastasis.

Disclosures

All authors state that they have no conflicts of interest.

Acknowledgments

References

1. Hofbauer LC, Rachner TD, Coleman RE, Jakob F. Endocrine aspects of bone metastases. Lancet Diabetes Endocrinol. 2014;2(6):500–12.

2. Clemons M, Gelmon KA, Pritchard KI, Paterson AHG. Bone-targeted agents and skeletal-related events in breast cancer patients with bone metastases: the state of the art. Curr Oncol. 2012;19(5):259–68.

3. Gómez García S, Clemons M, Amir E. Rethinking end-points for bone-targeted therapy in advanced cancer. Eur J Cancer. 2016;63:105–9.

4. Brook N, Brook E, Dharmarajan A, Dass CR, Chan A. Breast cancer bone metastases: pathogenesis and therapeutic targets. Int J Biochem Cell Biol. 2018;96:63–78.

5. Rosen LS, Gordon D, Kaminski M, et al. Long-term efficacy and safety of zoledronic acid compared with pamidronate disodium in the treatment of skeletal complications in patients with advanced multiple myeloma or breast carcinoma: a randomized, double-blind, multicenter, comparative trial. Cancer. 2003;98(8):1735–44.

6. Rosen LS, Gordon D, Tchekmedyian NS, et al. Long-term efficacy and safety of zoledronic acid in the treatment of skeletal metastases in patients with nonsmall cell lung carcinoma and other solid tumors: a randomized, phase III, double-blind, placebo-controlled trial. Cancer. 2004;100(12):2613–21.

7. Fizazi K, Carducci M, Smith M, et al. Denosumab versus zoledronic acid for treatment of bone metastases in men with castration-resistant prostate cancer: a randomised, double-blind study. Lancet. 2011;377(9768):813–22.

8. Lipton A, Fizazi K, Stopeck AT, et al. Effect of denosumab versus zoledronic acid in preventing skeletal-related events in patients with bone metastases by baseline characteristics. Eur J Cancer. 2016;53:75–83.

9. Stopeck AT, Lipton A, Body J-J, et al. Denosumab compared with zoledronic acid for the treatment of bone metastases in patients with advanced breast cancer: a randomized, double-blind study. J Clin Oncol. 2010;28(35):5132–9.

10. Cook GJR, Azad GK, Goh V. Imaging bone metastases in breast cancer: staging and response assessment. J Nucl Med. 2016;57(Suppl 1):27S–33S.

11. Goyal N, Kalra M, Soni A, Baweja P, Ghonghe NP. Multi-modality imaging approach to bone tumors—state-of-the art. J Clin Orthop Trauma. 2019;10(4):687–701.

12. Koizumi M, Matsumoto S, Takahashi S, Yamashita T, Ogata E. Bone metabolic markers in the evaluation of bone scan flare phenomenon in bone metastases of breast cancer. Clin Nucl Med. 1999;24(1):15–20.

13. Kang Y. Dissecting tumor-stromal interactions in breast cancer bone metastasis. Endocrinol Metab (Seoul). 2016;31(2):206–12.

14. Jeong HM, Cho SW, Park SI. Osteoblasts are the centerpiece of the metastatic bone microenvironment. Endocrinol Metab. 2016;31(4):485–92.

15. Buenrostro D, Park SI, Sterling JA. Dissecting the role of bone marrow stromal cells on bone metastases. Biomed Res Int. 2014;2014:875305.

16. Shiozawa Y, Pedersen EA, Havens AM, et al. Human prostate cancer metastases target the hematopoietic stem cell niche to establish footholds in mouse bone marrow. J Clin Invest. 2011;121(4):1298–312.

17. Shiozawa Y, Pienta KJ, Taichman RS. Hematopoietic stem cell niche is a potential therapeutic target for bone metastatic tumors. Clin Cancer Res. 2011;17(17):5553–8.

18. Mundy GR. Metastasis to bone: causes, consequences and therapeutic opportunities. Nat Rev Cancer. 2002;2(8):584–93.

19. Weilbaecher KN, Guise TA, McCauley LK. Cancer to bone: a fatal attraction. Nat Rev Cancer. 2011;11(6):411–25.

20. Park SI, Lee C, Sadler WD, et al. Parathyroid hormone-related protein drives a CD11b+Gr1+ cell-mediated positive feedback loop to support prostate cancer growth. Cancer Res. 2013;73(22):6574–83.

21. Park SI, Liao J, Berry JE, et al. Cyclophosphamide creates a receptive microenvironment for prostate cancer skeletal metastasis. Cancer Res. 2012;72(10):2522–32.

22. Eghbali-Fatourechi GZ, Lamsam J, Fraser D, Nagel D, Riggs BL, Khosla S. Circulating osteoblast-lineage cells in humans. N Engl J Med. 2005;352(19):1959–66.

23. Eghbali-Fatourechi GZ, Mödder UIL, Charatcharoenwitthaya N, et al. Characterization of circulating osteoblast lineage cells in humans. Bone. 2007;40(5):1370–7.

24. Suda RK, Billings PC, Egan KP, et al. Circulating osteogenic precursor cells in heterotopic bone formation. Stem Cells. 2009;27(9):2209–19.

25. Pal SN, Rush C, Parr A, Van Campenhout A, Golledge J. Osteocalcin positive mononuclear cells are associated with the severity of aortic calcification. Atherosclerosis. 2010;210(1):88–93.

26. Undale A, Srinivasan B, Drake M, et al. Circulating osteogenic cells: characterization and relationship to rates of bone loss in postmenopausal women. Bone. 2010;47(1):83–92.

27. Rubin MR, Manavalan JS, Dempster DW, et al. Parathyroid hormone stimulates circulating osteogenic cells in hypoparathyroidism. J Clin Endocrinol Metab. 2011;96(1):176–86.

28. Egan KP, Duque G, Keenan MA, Pignolo RJ. Circulating osteogenetic precursor cells in non-hereditary heterotopic ossification. Bone. 2018;109:61–4.

29. Pettaway CA, Pathak S, Greene G, et al. Selection of highly metastatic variants of different human prostatic carcinomas using orthotopic implantation in nude mice. Clin Cancer Res. 1996;2(9):1627–36.

30. Park SI, Kim SJ, McCauley LK, Gallick GE. Pre-clinical mouse models of human prostate cancer and their utility in drug discovery. Curr Protoc Pharmacol. 2010 Chapter 14:Unit14.15.

31. Lee C, Whang YM, Campbell P, et al. Dual targeting c-met and VEGFR2 in osteoblasts suppresses growth and osteolysis of prostate cancer bone metastasis. Cancer Lett. 2018;414:205–13.

32. Cho SW, Soki FN, Koh AJ, et al. Osteal macrophages support physiologic skeletal remodeling and anabolic actions of parathyroid hormone in bone. Proc Natl Acad Sci U S A. 2014;111(4):1545–50.

33. Feehan J, Nurgali K, Apostolopoulos V, Saedi Al A, Duque G. Circulating osteogenic precursor cells: building bone from blood. EBioMedicine. 2019;39:603–11.

34. D'Oronzo S, Brown J, Coleman R. The value of biomarkers in bone metastasis. Eur J Cancer Care. 2017;26(6):e12725.

35. Coleman R, Brown J, Terpos E, et al. Bone markers and their prognostic value in metastatic bone disease: clinical evidence and future directions. Cancer Treat Rev. 2008;34(7):629–39.

36. D'Oronzo S, Brown J, Coleman R. The role of biomarkers in the management of bone-homing malignancies. J Bone Oncol. 2017;9:1–9.

37. Shanmugam MK, Ahn KS, Hsu A, et al. Thymoquinone inhibits bone metastasis of breast cancer cells through abrogation of the CXCR4 signaling axis. Front Pharmacol. 2018;9:1294.

38. Tulotta C, Ottewell P. The role of IL-1B in breast cancer bone metastasis. Endocr Relat Cancer. 2018;25(7):R421–34.

39. Huang S, Zou C, Tang Y, et al. miR-582-3p and miR-582-5p suppress prostate cancer metastasis to bone by repressing TGF-β signaling. Mol Ther Nucleic Acids. 2019;16:91–104.

40. Pavlovic M, Arnal-Estapé A, Rojo F, et al. Enhanced MAF oncogene expression and breast cancer bone metastasis. J Natl Cancer Inst. 2015;107(12):djv256.

41. Pineda Moncusí M, Garcia Giralt N, Diez Perez A, et al. Increased fracture risk in women treated with aromatase inhibitors versus tamoxifen: beneficial effect of bisphosphonates. J Bone Miner Res. 2019;11 (12):1135–7.